Statistics of Echoes From a Directional Sonar Beam Insonifying Finite Numbers of Single Scatterers and Patches of Scatterers

Article *in* IEEE Journal of Oceanic Engineering · May 2010

DOI: 10.1109/JOE.2009.2037988 · Source: IEEE Xplore

Statistics of Echoes From a Directional Sonar Beam Insonifying Finite Numbers of Single Scatterers and Patches of Scatterers

Dezhang Chu and Timothy K. Stanton

***Abstract*—When a sonar beam sweeps across a field of scatterers and insonifies a different set of scatterers in each ping, the echoes can fluctuate significantly from ping to ping. For a homogeneous spatial distribution of scatterers in which there are a large number of scatterers in each sonar resolution cell, the echoes tend to be Rayleigh distributed. However, the echoes can be strongly non-Rayleigh when there is a small number of scatterers in the sonar resolution cell—a condition that can occur with a narrow beam sonar. For scatterers randomly distributed in the sonar beam, the corresponding random weighting associated with the beampattern also significantly contributes toward a non-Rayleigh distribution when the number of scatterers is small. In this paper, a general formulation for echo statistics is developed by combining equations derived by Ehrenberg *et al.* [*Proc. Conf. Eng. Ocean Environ.*, vol. 1, pp. 61–64, 1972 and *J. Acoust. Soc. Amer.*, vol. 69, pp. 955–962, 1981] and Barakat [*Optica Acta*, vol. 21, pp. 903–921, 1974] to account for a directional sonar beam involving an arbitrary finite number of scatterers, each with an arbitrary echo probability density function (pdf), each randomly located in the beam, and each correspondingly randomly weighted by the beampattern. Theoretical predictions are made, along with numerical simulations for validation, for a range of cases including: 1) a range of number of scatterers each randomly located in the beam and 2) several different echo pdfs of the scatterers. Here, a "single scatterer" could be a patch of scatterers whose overall dimensions are much smaller than the resolution cell of the sonar beam and multiple scatterers could be multiple small patches. Although the application is intended for volumetric patches, the formulation could be applied to areal patches under appropriate conditions. The formulation applies directly to the geometry of the short-range direct-path sonar in which there are no reflections due to boundaries such as the seafloor and sea surface.**

***Index Terms*—Beampattern, echo statistics, scattering, sonar.**

Manuscript received January 29, 2009; revised October 07, 2009; accepted November 03, 2009. Date of publication March 29, 2010; date of current version May 26, 2010. This work was supported by the U.S. Office of Naval Research (ONR) under Grants N00014-06-1-0197 and N00014-07-1-0232.

Associate Editor: D. A. Abraham.

D. Chu was with the Woods Hole Oceanographic Institution, Woods Hole, MA 02543 USA. He is now with the National Marine Fisheries Service, National Oceanic and Atmospheric Administration (NOAA), Seattle, WA 98112 USA.

T. K. Stanton is with the Department of Applied Ocean Physics and Engineering, Woods Hole Oceanographic Institution, Woods Hole, MA 02543 USA (e-mail: tstanton@whoi.edu.)

Color versions of one or more of the figures in this paper are available online at http://ieeexplore.ieee.org.

Digital Object Identifier 10.1109/JOE.2009.2037988

I. Introduction

NATURALLY occurring objects or processes in the ocean are inherently inhomogeneous or "patchy" in space. For example, marine organisms will aggregate according to a combination of schooling behavior and local environmental conditions (which is also inhomogeneous) [1], [2]. Features on the seafloor such as rock outcrops will result from the local inhomogeneous geological processes [3]. For these and other reasons discussed below involving beampattern and echo interference effects, echoes from directional sonars whose beams are scanning an area and insonify a different set of scatterers in each ping will significantly fluctuate from ping to ping.

A key aspect to the statistical characteristics of the echoes is the degree to which they are non-Rayleigh. For example, for a finite number of scatterers or patches of scatterers insonified in any given ping, the echoes may be non-Rayleigh with high tails in the echo amplitude histogram. The degree to which the statistics are non-Rayleigh depends upon how few scatterers or patches there are in the beam. The fewer the scatterers or patches, the more the statistics will deviate from Rayleigh statistics. This condition of few scatterers or patches is more likely to occur with directional sonars with small resolution cells [4]–[8].

For sonars whose purpose is to detect targets of interest in the presence of naturally occurring scatterers, those naturally occurring scatterers may be a source of interference or "clutter." The interference is especially problematic when it is non-Rayleigh distributed as the tails of the distribution are high compared with Rayleigh-distributed echoes. This non-Rayleigh nature of the echoes needs to be accounted for to reduce the probability of false alarm (see, for example, [9]). For sonars whose purpose is to study naturally occurring scatterers, the statistical characteristics of the echoes can, in principle, be interpreted in terms of meaningful quantities [5]. For example, the transition from Rayleigh to non-Rayleigh echo amplitude distributions has been used to estimate the numerical density of fish [10] and zooplankton [11]. While each of the above cases has different motivations, that is, in the former case, the scattering by the natural objects is a source of interference or "noise" and in the latter case, the scattering is the "signal" of interest, characterization of the statistics of the echoes in each of the cases is generally similar, if not identical.

Predicting echo statistics associated with fields of naturally occurring scatterers is quite complex. The predictions can be divided into three broad categories of increasing complexity, most of which is reviewed in [5].

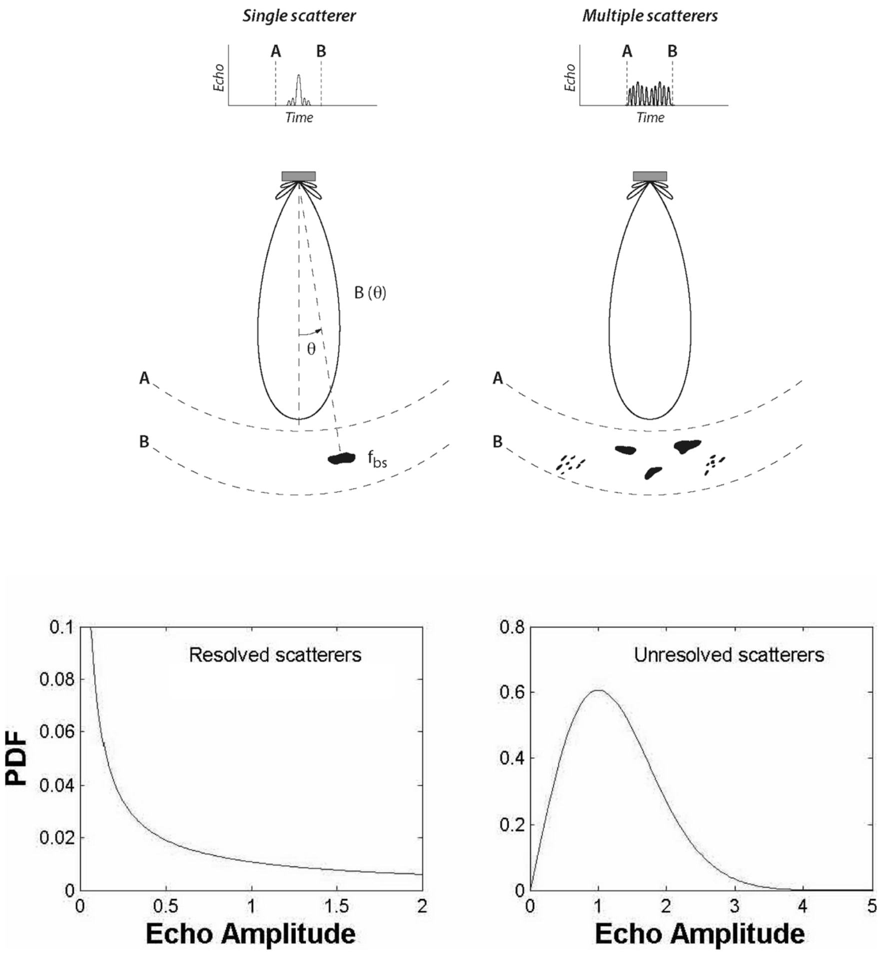

Fig. 1. Effects of beampattern on echo envelope pdf for two limiting cases. Left column: A strongly non-Rayleigh pdf results from the scatterer being resolved within a beam. Here the echo pdf is the convolution of the pdf associated with the scatterer being randomly located in the beam (and, hence, randomly weighted by the beam) and the pdf of the scattering amplitude of the scatterer. Right column: Once there are many unresolved scatterers in the beam, the result tends to a Rayleigh pdf. Curves taken from [5].

1) Single scatterer, no beampattern effects. The echo from a single scatterer in an omnidirectional beam can fluctuate from ping to ping (or, more precisely, from realization to realization) as the scatterer changes shape and/or orientation.
2) Multiple scatterers, no beampattern effects. The echo from multiple scatterers in an omnidirectional beam can fluctuate from ping to ping as the scatterers not only change shape and/or orientation, but also change their relative distance from the sonar which, in turn, changes their relative phase shifts. Typically, the phase shift of the narrowband components of the echoes from individual scatterers is randomly and uniformly distributed over the range 0–2π and will vary independently from ping to ping. For this case, and for the case of the limit of a very large number of scatterers, the echoes will tend to be Rayleigh distributed [12]–[14].
3) Beampattern effects (Fig. 1). In the simplest case, for a point scatterer whose echo distribution is a delta function probability density function (pdf) (without including beampattern effects), the echo will fluctuate significantly from ping to ping as the scatterer moves across a directional sonar beam (left column of Fig. 1). For a narrow beam, a randomly located scatterer will spend most of the time in the sidelobes and side of the mainlobe, which are all rapidly varying quantities, resulting in strongly non-Rayleigh echoes (lower left panel of Fig. 1). Here, the location of the scatterer in the beam or, more precisely, the angle relative to the center of the mainlobe, is a random variable. Although the beampattern is not random, since it depends upon the random angle, then the beampattern weighting factor in the context of this analysis is a random variable. This randomized weighting factor is referred to, compactly, as the "beampattern pdf." For the more complex case of multiple scatterers in a beam, the weighting of the beam can reduce the effective number of scatterers to perhaps a smaller number (right column of Fig. 1). Without the beam, the echoes due to many insonified scatterers may be Rayleigh distributed, however with a directional beam and possibly only several scatterers effectively insonified, the echo pdf may transition into a non-Rayleigh distribution. In the limit of a very large number of scatterers in the sonar beam, the pdf will tend to the Rayleigh distribution as shown in the lower right panel of Fig. 1.

There has been much research in the area of echo statistics, including systematic studies comparing a variety of statistical distributions to data (see, for example, [15]–[17]) and other studies where parameters of certain distributions were connected to numbers of scatterers and sonar parameters (see, for example, [5] and [6]). Although much insight was derived from those studies, a unifying formulation was lacking that explicitly accounts for both an arbitrary field of scatterers and beampattern effects.

In this paper, a general formula is derived describing the echo pdf due to an arbitrary number of scatterers randomly located in a directional sonar beam. The scattering geometry involves the direct-path case in which there are no reflections from neighboring boundaries such as the seafloor or sea surface. Each scatterer can have an arbitrary echo pdf (before beampattern effects) and the number of scatterers can range from one to an arbitrarily large number. The work builds upon that of Ehrenberg (and colleagues) who derived a general formula which incorporates the beampattern pdf into the echo pdf for a single resolved scatterer [18], [19]. The echo from a single scatterer (including beampattern effects) in Ehrenberg's formulation is treated as a random variable. This single-scatterer random variable is summed in this paper for an arbitrary number of independent unresolved arbitrary scatterers, each randomly located in the beam, through the method derived by Barakat [20] which makes use of characteristic functions. The resultant echo pdf formula, in addition to being general, is connected directly to the number of, and statistical characteristics of, the scatterers as well as to sonar parameters. Also, "scatterers" in this formulation can be either individuals or patches of scatterers whose overall dimensions are much smaller than the footprint of the sonar beam.

The new general formulation is used to predict echo pdfs for various combinations of scatterers or patches of scatterers with and without beampattern effects and over a wide range of (fixed) numbers of scatterers. In all examples, the field of scatterers or patches is assumed to be randomly and uniformly distributed in space. Numerical simulations are also made to validate the predictions. In addition, the beampattern pdf is investigated. Ehrenberg derived a simple power-law expression to describe the pdf and he numerically determined the slope of the power law for narrow beams. In this paper, an analytical expression is derived for the slope that is valid over a wide range of beamwidths.

II. Echo PDFs for Multiple Scatterers —No Beampattern Effects

Here, the echoes from the scatterers are treated as complex random variables. The echo pdf depends strongly upon the number of scatterers as well as the statistical properties of the echo from each scatterer. For the classic case of an infinite number of unresolved scatterers, the magnitude of the complex echo is Rayleigh distributed. Once the number of scatterers becomes finite, the predictions are more complex. Below is a brief description of the Rayleigh distribution and two other formulations (K-distribution [21] and the formulation by Barakat [20]) involving a finite number of scatterers. All formulations involve the summation of complex random variables (echoes from individual scatterers) without explicitly accounting for a beampattern. In Section III, beampattern effects, as predicted by Ehrenberg for single scatterers in [18] and [19], will be incorporated into Barakat's formula for a finite number of scatterers. Then, effects of the beampattern on delta-function-distributed, Rayleigh-distributed, and K-distributed scatterers will be illustrated.

A. Infinite Number of Scatterers: Rayleigh Distribution

For the case of an infinite number of scatterers, the magnitude of the complex echo is Rayleigh distributed

$$p_R(\tilde{e}) = \left(\frac{\tilde{e}}{\sigma^2}\right) e^{-\tilde{e}^2/2\sigma^2} \tag{1}$$

where $\tilde{e}$ is the magnitude of the echo and σ is a parameter proportional to the mean [12]–[14]. This expression, which results from the central limit theorem, can be derived by assuming that the real and imaginary parts of the echo are independently Gaussian with a mean of zero and variance of σ^2. For the common case of a narrowband signal, this corresponds to the phase of the echo from each scatterer being assumed to be randomly and uniformly distributed in the range 0–2π. The envelope amplitude of the summation of the random phase sinusoids is Rayleigh distributed in this narrowband case.

B. Finite Number of Scatterers: Method of Characteristic Functions

For the case of a finite number of scatterers where the echo pdf from each scatterer is arbitrary and can be different from each other, Barakat used characteristic functions (CFs) to provide an analytical expression of the pdf of the magnitude of the complex echo from the summed echoes [20]

$$p_A^{\Sigma}(\tilde{e}) = 2\tilde{e}\sum_{m=1}^{\infty}\frac{\phi_{R,I}^{\Sigma}\left(\frac{\eta_m}{\tilde{e}_{\max}}\right)}{[\tilde{e}_{\max}J_1(\eta_m)]^2}J_0\left(\eta_m\frac{\tilde{e}}{\tilde{e}_{\max}}\right) \tag{2}$$

where $\phi_{R,I}^{\Sigma}(\omega)$ is the CF of the real or imaginary component of the complex echo due to the summation of N scatterers, $J_\nu(x)$ is the Bessel function of the first kind of order ν, η_m ($m = 1, 2, \ldots$) are the positive roots of $J_0(x) = 0$, and $\tilde{e}_{\max}$ is the maximum echo amplitude. The summation over m involves the zeroes of the Bessel function, not the number of scatterers. Note that (2) is from [20, eq. (55)] (rewritten in terms of p_A) and p_A and $\tilde{e}$ correspond to $W(r)$ and r, respectively, in [20, eq. (56)]. In this approach, Barakat exploited the fact that the CF and pdf of a random variable are a Fourier transform pair and that the pdf of the sum of random variables can be calculated by the product of their respective CFs. Beampattern effects are not included in this formulation.

The characteristic function of the summed signal $\phi_{R,I}^{\Sigma}$ in (2) is the product of the individual CFs $\phi_{R,I}(\omega, \beta_n)$

$$\phi_{R,I}^{\Sigma}(\omega) = \prod_{n=1}^{N}\phi_{R,I}(\omega;\beta_n) \tag{3}$$

where $\phi_{R,I}(\omega;\beta_n)$ is the real or imaginary component of the characteristic function of the nth signal (scatterer) and β_n is the parameter vector for the nth characteristic function.

The pdf of one component of the summed complex signal is the inverse Fourier transform of the product of the corresponding CFs. However, since the signal is a two-component (complex) random variable, then the CFs of the real and imaginary components are first calculated to construct the magnitude

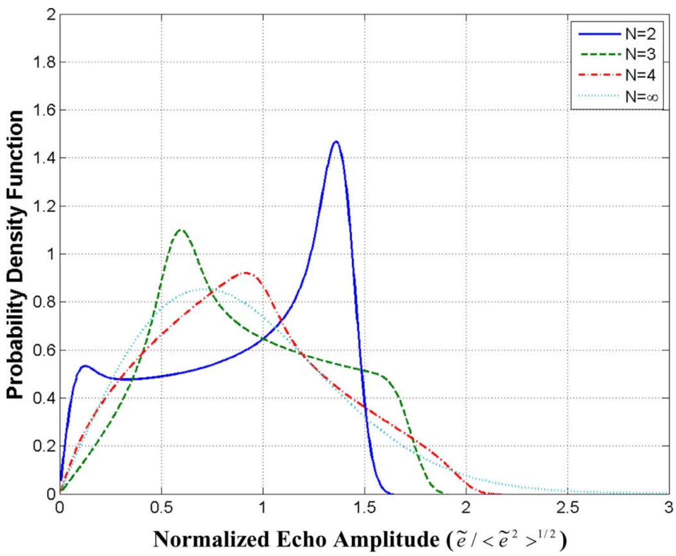

Fig. 2. The pdfs of magnitude of signal due to sums of N identical random variables, where $N = 2 - 4$ and infinity (approximated by $N = 100$ in calculations). Curves taken from [23] whose analysis is based on equations from [20] [see (2)].

of the complex signal. The CFs of the two components are identical. Then, Barakat used a projection approach to express the CF of the echo component (real or imaginary) of the nth scatterer in terms of the pdf $p_{A_n}(\tilde{e})$ of the magnitude of the echo of the nth scatterer through the integral

$$\phi_{R,I}(\omega;\beta_n) = \int_0^\infty p_{A_n}(\tilde{e})\, J_0(\omega\,\tilde{e}) d\tilde{e}. \tag{4}$$

This equation is from [20, eq. (21)] with p_{A_n} corresponding to f_a in that paper. Through mathematical manipulations, the pdf of the summed signal was reduced to a summation with respect to zeroes of the J_0 Bessel function, as shown in (2) (sum over m). Note that although the focus of Barakat's work was for narrowband signals, his formulation applies to the more general broadband case as explicitly stated in his paper.

Equation (2) is quite general. Through the method of (one-component) characteristic functions and accounting for the fact that complex signals have two components, the pdf of the magnitude of the complex echo from N summed arbitrary random signals in (2) is related to the pdf of the magnitude of each nth complex signal through (3) and (4). As stated above, N and the individual pdfs are arbitrary. This model was later extended by Jao and Elbaum to include a diffuse component that has a Rayleigh pdf, representing the background noise [22]. Example calculations of (2) are given in Fig. 2. The predictions illustrate the degree to which amplitude pdfs due to the summation of identical random variables are non-Rayleigh for small numbers of signals.

C. Finite Number of Scatterers: K-Distribution

Another approach to the problem was proposed by Jakeman and Pusey to describe non-Rayleigh distributions [21]. In their model, the pdf of the echo amplitude is

$$p_A(\tilde{e}) = \frac{4}{\sqrt{\lambda}\Gamma(\alpha)}\left(\frac{\tilde{e}}{\sqrt{\lambda}}\right)^\alpha K_{\alpha-1}\left(\frac{2\tilde{e}}{\sqrt{\lambda}}\right) \tag{5}$$

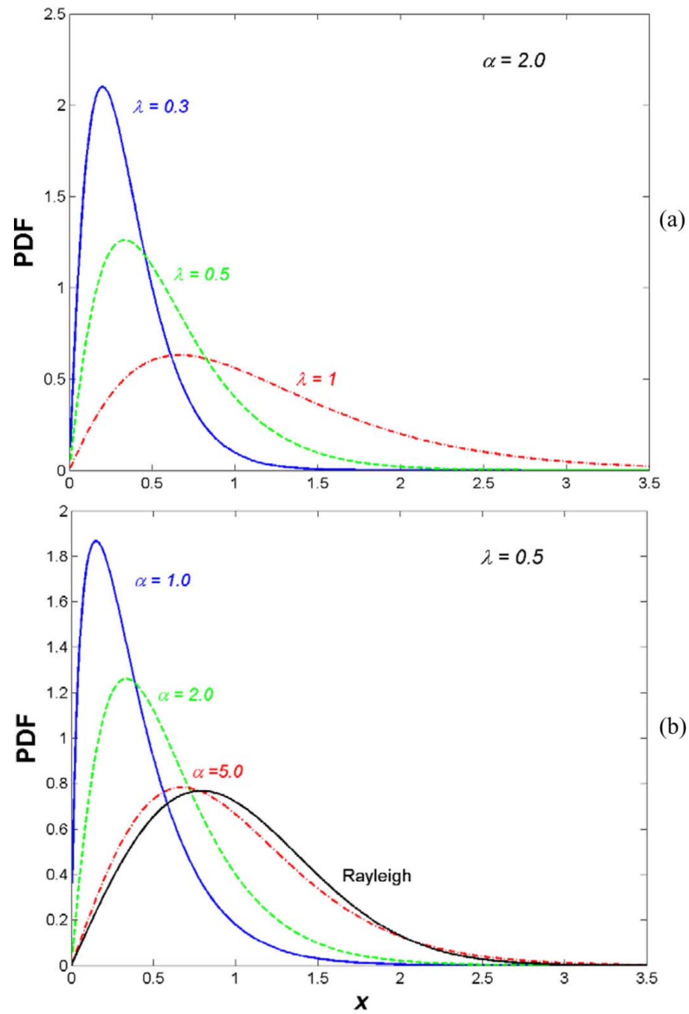

Fig. 3. K-distribution with different combinations of parameters: (a) fixed α, and (b) fixed λ. The Rayleigh pdf is superimposed in (b) for comparison since the K-distribution approaches the Rayleigh in the limit of high α.

where K is the modified Bessel function of the third kind (which inspired the naming of the distribution). After the introduction of the K-distribution, many applications and extensions based on Jakeman and Pusey's original work have been reported to describe waves scattered from different types of clutter, including radar echoes from the sea surface and land, laser echoes from a turbulent layer of nematic liquid crystal, ultrasound echoes from tissue, and sonar echoes from the seafloor [24]–[26]. Examples of the K-distribution are given in Fig. 3 for various combinations of parameters.

The K-distribution given by (5) can be derived based on a negative binomial distribution resulting from a 2-D random walk [27]. A more generalized K-distribution involving an n-dimensional random walk was later proposed in [28]. However, the derivations are quite complicated and physical interpretations in terms of scattering characteristics were indirect. In a recent paper by Abraham and Lyons, a more direct physical interpretation to the K-distributed random process was provided [6]. By assuming that the echoes from the scatterers were exponentially distributed, they related the number of scatterers to one of the parameters of the pdf ("α" in their work). This has proven to be a useful interpretation, although limited to this particular distribution of scatterers and not including beampattern effects.

III. PDF Models That Include Beampattern Effects

The echo received by a directional sonar system is a complex function of the statistical fluctuations due to each individual scatterer (before beampattern effects are accounted for), the number of scatterers, and their locations in the beam. For an individual resolved scatterer randomly located in the beam, the pdf of the beampattern has been used to predict the echo statistics [5], [18], [19], [29]. In this section, previously published equations accounting for beampattern effects are first reviewed. An analytical expression for the slope of the tail of the beampattern pdf is then derived, which greatly facilitates its calculation over the numerical approach that had been used previously. Using both general and simplified forms of beampattern pdf, the formulation predicting the echo statistics for single resolved scatterers is used to describe the echo statistics of the general case of an arbitrary number of unresolved scatterers or patches of scatterers randomly located in the beam, through the use of Barakat's formula given earlier.

A. Beampattern PDF

For a scatterer randomly located in a sonar beam, its echo will fluctuate from location to location according to the value of the beampattern at each location (left column of Fig. 1). Specifically, and for the case of a beampattern that is symmetric about its major response axis, the polar angle θ is a random variable. Although the beampattern itself is not random, it is a function of a random variable. As a result, the beampattern becomes a random variable in this application. Hence, it is important to calculate the "beampattern pdf" to describe the statistics of echoes from objects randomly located in the beam. A general solution not specific to this application for describing the pdf of a function of a random variable is given in [14]. Ehrenberg applied that general solution to this case of an axisymmetric beampattern to calculate the beampattern pdf

$$p_B(b) = \frac{p_\Theta\left(\theta(b)\right)}{\left|\dfrac{db}{d\theta}\right|_{\theta(b)}} \tag{6}$$

where b is the value of the beampattern $(0 \le b \le 1)$, θ is a random variable representing the spherical polar angle relative to the center of the axisymmetric beam, and p_Θ is the pdf of the scatterer position (θ). Formulas for calculating the beampattern pdf were first derived by Ehrenberg in [18], then further developed in [29] and [19] and reviewed in [5] and [30].

A key element in (6) is the derivative in the denominator. Here, the probability of occurrence of any given value of b is related inversely to the slope of $b(\theta)$. This slope, in combination with the numerator and, as illustrated on the left-hand side of Fig. 1 and given in detail later, results in the beampattern pdf assuming higher values for the lower values of b. That is, for an object randomly and uniformly located in the sonar beam, it will generally spend more time in the side of the mainlobe and in the sidelobes than in the center of the beam.

For a piston transducer with a radius of a and in a monostatic (backscattering) configuration, the (two-way) beampattern is

$$b = \left(\frac{2J_1(ka\sin\theta)}{ka\sin\theta}\right)^2 \tag{7}$$

where k is the acoustic wave number and $J_1(x)$ is the Bessel function of order 1 [31]. Assuming the scatterer is randomly and uniformly distributed in space across the sonar beam, the resultant pdf of the scatterer position in terms of the polar angle is

$$p_\Theta(\theta) = \sin\theta, \qquad 0 \le \theta \le \frac{\pi}{2}. \tag{8}$$

Substituting (7) and (8) into (6) gives

$$p_B(b) = \left.\frac{\sin^2\theta}{4\cos\theta\, J_2(ka\sin\theta)b^{1/2}}\right|_{\theta(b)}, \qquad b_{SL} \le b \le 1 \tag{9}$$

where b_{SL} is the value of the highest (first) sidelobe of the beampattern. Since b is multivalued for $b \le b_{SL} = 0.0175$, a general analytical form of $p_B(b)$ for all values of $b(0 \le b \le 1)$ is not practical. Thus, this equation and subsequent analytical forms of a power law (and the magnitude of its slope γ to be defined later) used to approximate it are limited to the scatterer(s) being confined to the mainlobe of the beampattern at points higher than the highest sidelobe level.

In [18], plots of (9) were shown to have a constant slope on a log–log scale. Ehrenberg and colleagues proposed the following power-law pdf, based on those and other similar plots

$$p_B(b) = k_0 b^{-\gamma}, \qquad b_{SL} \le b \le 1 \tag{10}$$

where $k_0 = (1-\gamma)b_{SL}^{\gamma-1}(b_{SL}^{\gamma-1}-1)^{-1}$ is a constant to ensure the integral of (10) is unity [19]. The parameter γ was determined in that study numerically through fitting a straight line to the function given in (9) on a log–log plot. However, it is possible to determine γ analytically, as we demonstrate below.

To explore this further analytically beyond the above cited works, the substitution $x = ka\sin\theta$ is made to put (9) into the following form:

$$p_B(b) = \left.\left(\frac{x}{2ka}\right)^2\left[\sqrt{1-\left(\frac{x}{ka}\right)^2}\sqrt{b}\,J_2(x)\right]^{-1}\right|_{x(b)}. \tag{11}$$

For small x, keeping the first three terms of the Taylor series expansion of the beampattern in (7), and solving for $x(b)$, we obtain

$$x(b) \cong 2\left(3-\sqrt{9-12\left(1-\sqrt{b}\right)}\right). \tag{12}$$

The error introduced by the approximations in (12) is less than 0.6% for $x \le 2$. This equation is a convenient form of x for certain limiting conditions, although it is not used in the remainder of this derivation.

With some mathematical manipulations of (11), the magnitude γ of the slope of the tail of $p_B(b)$ on a log–log plot can be derived in an exact form as (Appendix)

$$\gamma = \left[\frac{x}{(ka)^2 - x^2} + \frac{J_3(x)}{J_2(x)}\right] \frac{bx^2}{8J_1(x)J_2(x)} + \frac{1}{2}. \qquad (13)$$

This new expression is exact for $x < x_{SL} = ka\sin\theta_{SL} \simeq 3.305$, where θ_{SL} is the angle within the mainlobe at which the level of the mainlobe equals the level of the highest (first) sidelobe, i.e., $b = b_{SL}$. This is to ensure that the beampattern is a single-valued function of x.

For the limiting case of $x \to 0$ or $b \to 1$, γ can be proven to be independent of b and is given approximately as (Appendix)

$$\gamma = \frac{d(\log_{10} p_B)}{d(\log_{10} b)} = \frac{5}{6} + \frac{2}{(ka)^2} \qquad (14)$$

which yields 0.83 in the limit of $ka \to \infty$ (narrow beams). Ehrenberg determined γ through least squares fits to numerically determined pdfs involving narrow beams [18], [19]. In his studies, he determined γ to be to within 0.5% of 0.895 for transducer beamwidths of 20° or less $(4\pi \leq ka \leq 8\pi)$, compared with the range 0.836–0.846 calculated analytically with (14). A distinct advantage of (13) and (14) over Ehrenberg's numerical approach is the ease with which γ is calculated (analytically versus numerically). Furthermore, the two equations are still valid for $x = 0$ $(b = 1)$, while the missing points at $b = 1$ in [19, Fig. A1] and the abrupt drop in beampattern pdf as $b \to 1$ in [32, Fig. 2] suggested some difficulties in numerical evaluations.

B. *Echo PDF for Single Scatterer or Small Patch of Scatterers in the Beam*

For a single scatterer or small patch of scatterers randomly located in the beam, the pdf of the echo is

$$p_E(\tilde{e}) = \int_{\tilde{e}}^{\infty} \frac{1}{x} p_s(x) p_B\left(\frac{\tilde{e}}{x}\right) dx, \qquad 0 \leq b \leq 1 \qquad (15)$$

where $p_s(x)$ is the pdf of the magnitude of the scattering amplitude of the scatterer or patch of scatterers not including the influence of the beampattern and $p_E(\tilde{e})$ corresponds to the distribution of echoes as "seen" through the sonar system, including the beampattern effects [5], [18], [19], [29]. In this case, the dimensions of the patch must be small compared with the footprint of the sonar beam so that it appears as a single scatterer. Equation (15) is exact and general, and is applicable to arbitrary scatterers and beampattern pdfs. This equation was derived by Ehrenberg by treating both the scattering amplitude and the beampattern as random variables [since the beampattern is a function of the (angular) location of the scatterer which is a random variable, then the beampattern, in turn, becomes a random variable]. The echo, as measured through the sonar system, is then the product of those two random variables. The pdf of the product is the convolution of the pdfs of the individual random variables and, through change of variables, Ehrenberg derived (15).

Incorporating (10) into (15) shows explicit (approximate) dependence upon parameters of the beampattern

$$p_E(\tilde{e}) = k_0 \tilde{e}^{-\gamma} \int_{\tilde{e}}^{\infty} x^{\gamma-1} p_s(x) dx, \qquad b_{SL} \leq b \leq 1 \quad (16)$$

where, as stated above, only the tail of the pdf of the beampattern, which corresponds to all portions of the mainlobe above the level of the highest sidelobe, is accounted for. Two examples are now given for the cases in which p_s is narrowly and Rayleigh distributed.

For an individual scatterer with a narrowly distributed scattering amplitude, such as a swimbladder-bearing fish insonified at its resonance frequency, $p_s(x) \approx \delta(x - \tilde{e}_0)$, where $\tilde{e}_0$ is the scattering amplitude of the fish swimbladder at resonance. In this case, (16) gives

$$p_E(\tilde{e}) = k_0\, \tilde{e}_0^{\gamma-1} \tilde{e}^{-\gamma}, \qquad b_{SL} \leq b \leq 1. \qquad (17)$$

If $p_s(x)$ follows a Rayleigh pdf $(p_s(x) = (x/\sigma^2)\, e^{-x^2/2\sigma^2})$, such as in the cases of a single irregular scatterer at high frequencies or a small patch of many scatterers, the echo amplitude pdf using (16) is given in [19] as

$$p_E(\tilde{e}) = \frac{1}{2} k_0 \tilde{e}^{1-\gamma} \Gamma\left(\gamma + 1, \frac{\tilde{e}}{\sqrt{2}\sigma}\right), \qquad b_{SL} \leq b \leq 1 \quad (18)$$

where $\Gamma(\alpha, x)$ is the incomplete gamma function. This is a corrected version of what appears in [19].

Examples of the above two cases as well as the case in which the scatterer has a K-distribution scattering amplitude (before beampattern effects) are given in Fig. 4. Here, the effects of the beampattern on the echo statistics are most distinctly illustrated for the case in which the scatterer echo (before beampattern effects) is delta function distributed. In that case, the echo is transformed, through the effects of the beampattern, to a power-law distributed echo. In the other cases where the scatterer echo (before beampattern effects) is broadly distributed, the echo is transformed into one that is more heavily distributed near small values. The tails of pdfs will be examined more closely in Section III-C.

C. *Echo PDF for Finite Number of Scatterers Distributed Throughout the Beam*

The more general case of an arbitrary finite number (N) of scatterers distributed randomly throughout the beam is considered. As in the case above, each scatterer is either an individual or a small patch of scatterers whose overall dimensions are small compared with the footprint of the sonar beam. In this latter case, there would be N small patches of scatterers distributed randomly throughout the beam. The sonar echo pdf in this general case treats the echo from each scatterer (or patch) as a random variable, which includes its own inherent statistical properties (p_s) and the influence of the beampattern (p_B), according to (15) and (16). Using the approach of Barakat in [20], the sonar echo pdf can be calculated using (2), where $p_A^{\Sigma}(\tilde{e})$ in (2) notationally becomes $p_E^{\Sigma}(\tilde{e})$.

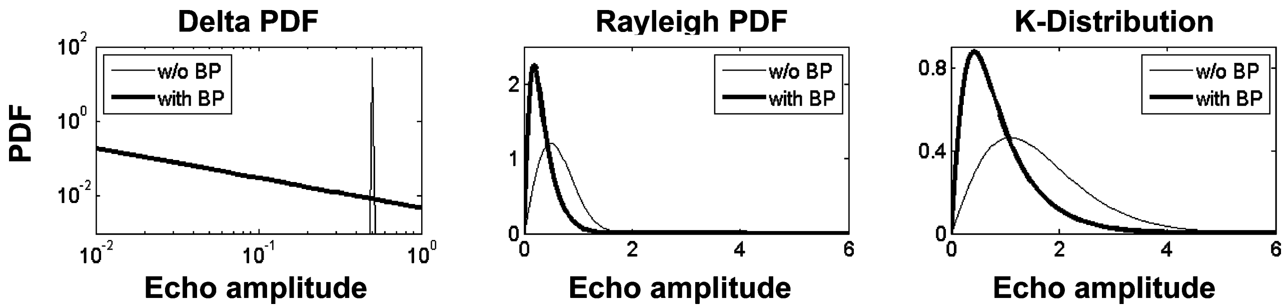

Fig. 4. Effects of beampattern for single resolved scatterer or patch of scatterers ($N = 1$). Examples are given, with and without beampattern effects, for the cases in which the pdf of the scatterer echo (before beampattern effects) is the delta function, the Rayleigh pdf, and the K-distribution. This analysis applies to the case for a single resolved scatterer randomly located in the beam or a small patch of unresolved scatterers (also randomly located in the beam) whose overall dimensions are small compared with the sonar footprint. The quantity ka (where a is the radius of the circular transducer) is equal to 2π for all calculations, which corresponds to a beamwidth of about 30°. The echo amplitude (horizontal axis) for each curve within a given panel is normalized by the root mean square echo before beampattern effects are accounted for. This allows for illustration of the shift in mean signal due to beampattern effects. Each pdf (vertical scale) is normalized in the usual manner so that the area under the curve is unity. In the far right panel, $\alpha = 4$ in the K-distribution. In each prediction involving beampattern effects, the pdf of the beampattern is assumed to follow a simple power law, using the limiting form of γ given in (14) and is incorporated into (17) (delta function pdf) or (16) (Rayleigh or K-distribution).

For the most general case, in which no approximations are made concerning the beampattern pdf, the nth component of $\phi^{\Sigma}_{R,I}(x)$ in (3) is calculated by inserting $p_E(\tilde{e})$ from (15) for each nth scatterer into $p_{A_n}(\tilde{e})$ of (4)

$$\phi_{R,I}(\omega, \beta_n) = \int_0^\infty \left(\int_{\tilde{e}}^\infty \frac{1}{x} p_{s_n}(x) p_B\left(\frac{\tilde{e}}{x}\right) dx \right) J_0(\omega\, \tilde{e}) d\tilde{e}, \quad 0 \le b \le 1. \quad (19)$$

Equation (19), in combination with (2) and (3), represents a general solution to predict the sonar echo pdf for N scatterers or N small patches of scatterers randomly and uniformly distributed throughout the beam. The solution is general enough to allow for a wide range of beamwidths as well as each scatterer or small patch of scatterers having an arbitrary and different echo pdf (p_{s_n}). Furthermore, it is exact, as the pdf $p_B(\tilde{e}/x)$ for the beampattern remains in general form.

Equation (19) can be written in a more explicit, but approximate, form by expressing the beampattern pdf in terms of the slope parameter γ. Replacing the inner integral of (19) [which is from (15)] with (16) gives

$$\phi_{R,I}(\omega, \beta_n) = \int_0^\infty \left(k_0 \tilde{e}^{-\gamma} \int_{\tilde{e}}^\infty x^{\gamma-1} p_{s_n}(x)\, dx \right) J_0(\omega\, \tilde{e}) d\tilde{e} \quad b_{SL} \le b \le 1 \quad (20)$$

$$= k_0 \int_0^\infty \tilde{e}^{-\gamma} t_n(\tilde{e}) J_0(\omega\, \tilde{e}) d\tilde{e} \quad (21)$$

where β_n represents a set of parameters of the nth CF including

$$t_n(\tilde{e}) = \int_{\tilde{e}}^\infty x^{\gamma-1} p_{s_n}(x)\, dx. \quad (22)$$

Although (20) is accurate, it is only valid for the case in which the scatterer is in the mainlobe at points higher than the highest sidelobe. Because of this approximation, (20) is only valid for the corresponding higher range of echo amplitudes (that is, the tail of the echo pdf).

Example calculations of echo pdfs involving the cases in which there are 2, 3, 4, and 100 scatterers or patches randomly distributed in the beam are given in Figs. 5 and 6. The plots involve predictions using the new formulation (solid lines) and numerical calculations ("0" and "*") for validation. The predictions use the exact form of the new formulation [(19) in combination with (2) and (3)] so accurate values of pdfs could be calculated for the entire range of echo amplitudes. The numerical calculations used a random number generator to calculate the random location (three dimensions) of each scatterer in the sonar beam. From that, the phase and amplitude (due to multiplication of the randomized scattering amplitude with the beampattern at that location) was calculated. The resultant echo for N scatterers, each randomly located in the beam, was the (narrowband) phasor addition of the complex signals. Both the theoretical predictions and numerical calculations used the exact beampattern given in (7) so that the pdf of the beampattern $p_B(b)$ could be determined exactly (numerically) for each set of computations. Since p_B was being determined numerically, the restriction of $b \ge b_{SL}$ did not apply as it did in the approximate analytical formulations, thus the value of b was made as close to 0 as practical (10^{-5} in this case) in the numerical calculations. Thus, in all calculations, the value of the beampattern was in the range $10^{-5} \le b \le 1$, where $b = 1$ corresponds to the center of the beam.

In Fig. 5, the echo from each scatterer or patch of scatterers in the beam is delta function distributed (before beampattern effects; each with the same mean). In Fig. 6, the echo from each scatterer or patch of scatterers in the beam is Rayleigh distributed (before beampattern effects; each with the same mean). In each case, when beampattern effects are accounted for, the echo pdfs are strongly non-Rayleigh, especially for small numbers of scatterers or patches of scatterers and even in the case in which the scatterers were Rayleigh-distributed before beampattern effects. For both small and high values of echo amplitude, the pdfs have significantly elevated values over the corresponding case without beampattern effects. The mode of the echo pdfs is also shifted down toward smaller values of echo value once beampattern effects are accounted for. This mode tends to shift toward higher values of echo value as the number of scatterers or patches is increased.

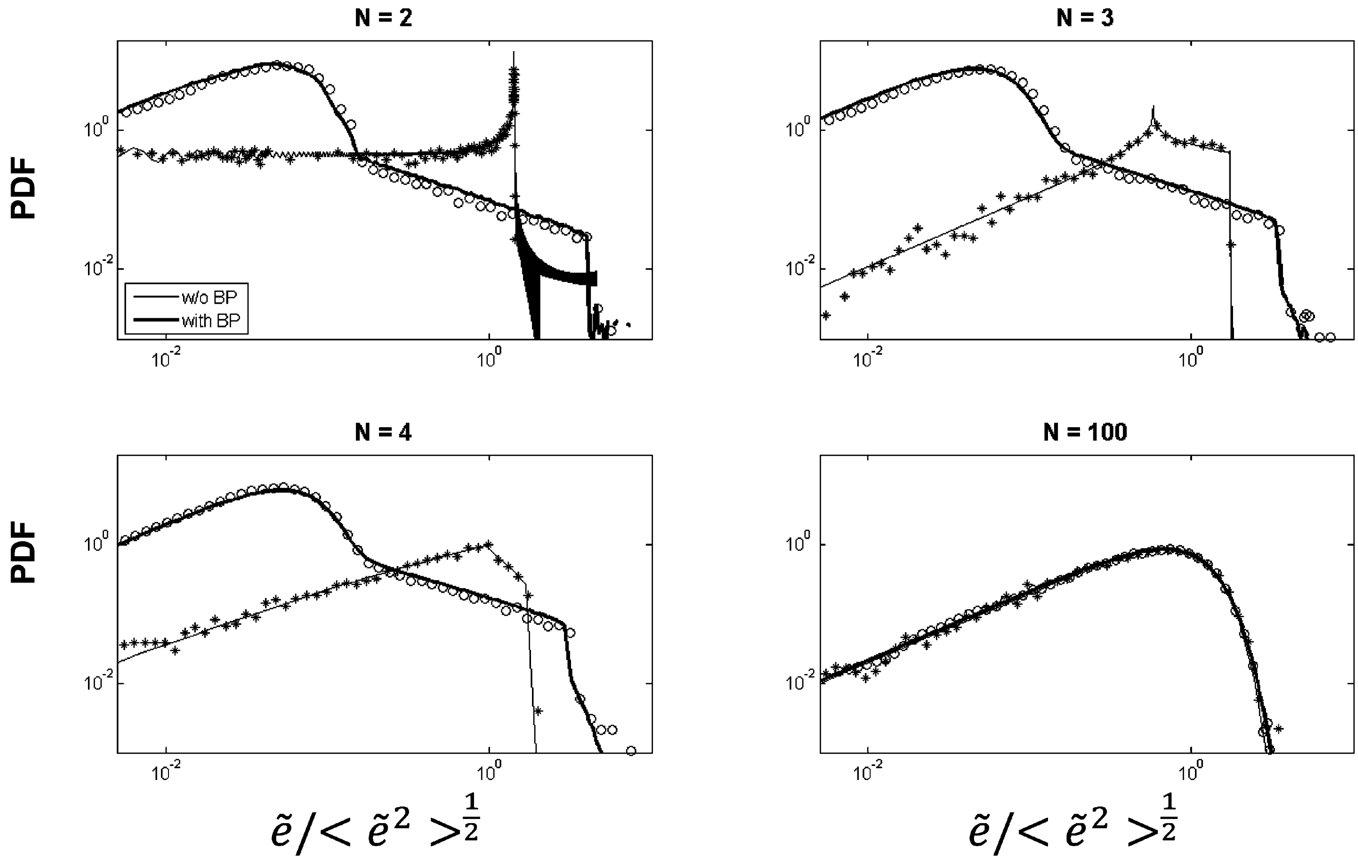

Fig. 5. Effects of beampattern for multiple unresolved scatterers, each randomly and independently located in the beam. The echo from each scatterer before beampattern effects is delta-function distributed, each with the same mean. Predictions (solid lines) using (2), (3), and (19) with the exact beampattern pdf ($10^{-5} \leq b \leq 1$) are compared with numerical simulations (symbols). Corresponding calculations are made for the case where there are no beampattern effects (i.e., omnidirectional beam) making direct use of Barakat's formulas in (2)–(4). Details on ka are the same as in caption to Fig. 4.

Overall, there was good agreement between the theoretical predictions using the new formulation and the numerical calculations. However, rigorous comparison between the two was not possible over the entire range of parameters since each set of calculations (using the formula or numerically based approach) has precision-related difficulties at low values of the pdf, low values of echo amplitude, and high values of N, as illustrated by the oscillatory nature of some of the plots. In some cases, the plot was cut off because of the numerical difficulties.

IV. Summary and Conclusion

Statistics of the echo from individual scatterers and small patches of scatterers are examined. Effects due to the sonar beampattern are taken into account for both resolved individuals and multiple unresolved scatterers. A formula is derived, based on the work of Ehrenberg and colleagues in [18] and [19], which (analytically) describes the tail of the beampattern pdf. Also, a general formulation is developed, combining the results of Ehrenberg and colleagues in [18] and [19] and those of Barakat in [20], which predicts the echo pdf as observed through the receiver of the sonar system for an arbitrary (finite) number of scatterers or patches of scatterers distributed randomly throughout the beam, each with their own scattering amplitude pdf. The new formulation is given both for exact and approximate forms of the beampattern pdf. Predictions based on this new formulation are validated through numerical simulations.

These results are significant because of the generality of the echo statistics formulation and the fact that there is a direct analytical connection between the echo statistics and the statistics of the scattering and sonar parameters. The echo statistics are related analytically to the echo pdf of each patch or scatterer (before beampattern effects), to the number of scatterers, as well as to the shape of the sonar beampattern. In addition, since the general formula does not require the scatterers or patches to be in the water column, the formula may also apply to scatterers (individuals or patches) to be on a boundary such as the sea surface or seafloor. In the former case, the patches would be 3-D or volumetric while in the latter cases they would be 2-D or areal.

Predictions based on this new formulation further quantify conditions under which echoes due to scatterers are non-Rayleigh. Clearly, the beampattern has a profound effect on the echo statistics. The echo pdf for individual resolved scatterers or patches randomly located in the beam was shown to be strongly non-Rayleigh, which is consistent with the results of previous studies. Furthermore, once there are multiple unresolved scatterers or patches, the echo remained strongly non-Rayleigh for small numbers of scatterers or patches. Whether the case involves individual resolved scatterers or patches, or multiple scatterers or patches, the beampattern significantly influenced the shape of the pdf until there were many

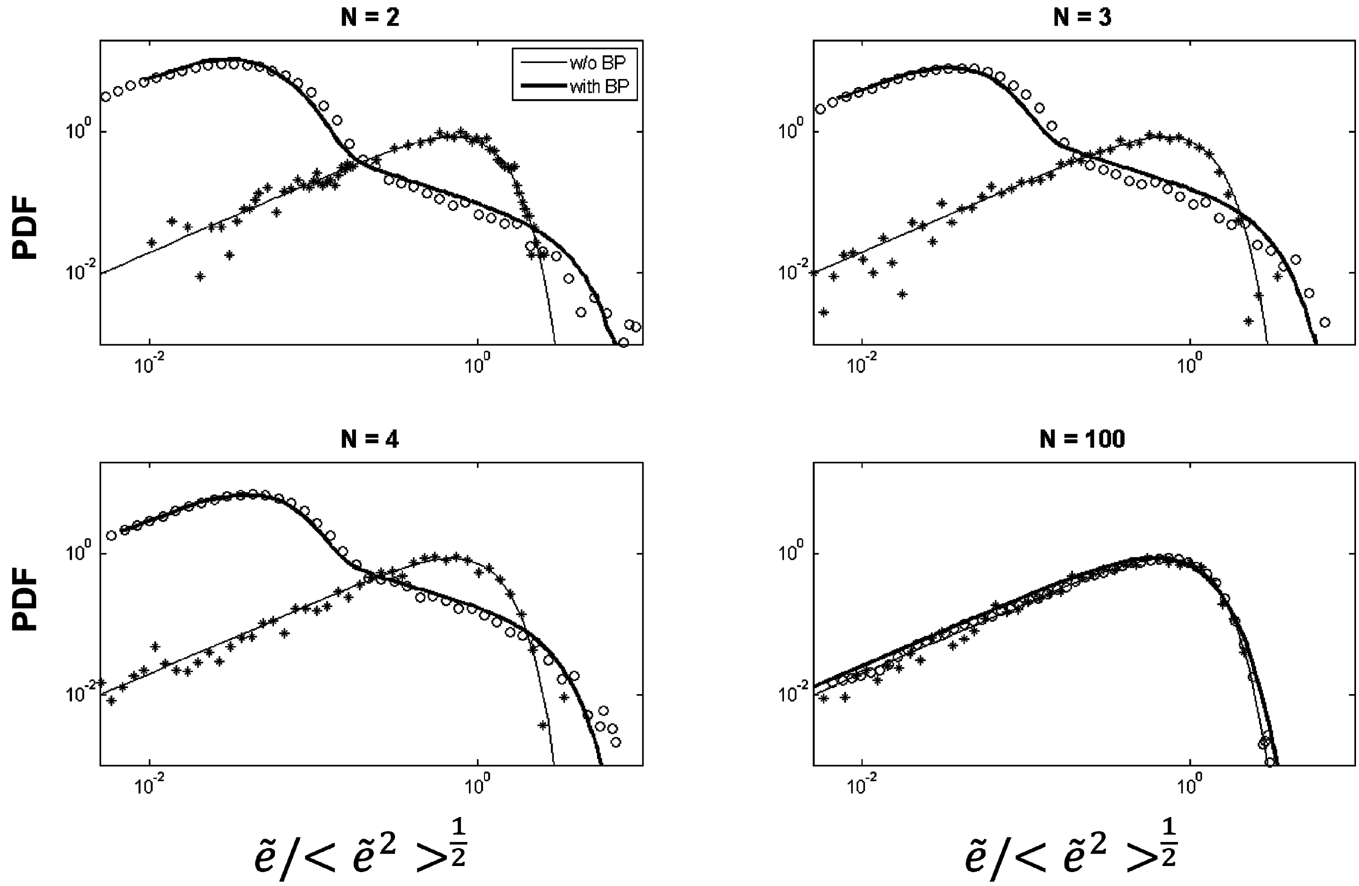

Fig. 6. Effects of beampattern for multiple unresolved scatterers, each randomly and independently located in the beam. The echo from each scatterer before beampattern effects is Rayleigh distributed, each with the same mean. Predictions (solid lines) using (2), (3), and (19) with the exact beampattern pdf ($10^{-5} \leq b \leq 1$) are compared with numerical simulations (symbols). Corresponding calculations are made for the case where there are no beampattern effects (i.e., omnidirectional beam) making direct use of Barakat's formulas in (2)–(4). Details on ka are the same as in caption to Fig. 4.

scatterers or patches in the beam and the echo pdf approached the Rayleigh, as expected (central limit theorem).

The predictions were limited to the cases of a noise-free system, with no diffuse (noise-like) or background scattering, and a direct-path geometry in which there were no reflections associated with boundaries such as the seafloor and sea surface. While accounting for those effects is outside the scope of this study, they can be significant. For example, in [33], an example was given where a two-component mixture pdf was required to account for the presence of resolved fish and background noise. One component was associated with the scattering by the fish [see (17)] and the other was associated with the background noise. In another study, Abraham showed how the pdf shape parameter of the echo changed with increasing number of paths in a multipath environment (ocean waveguide) [34]. In this case, the added paths "whitened" the signal in that it tended from non-Rayleigh toward Rayleigh with increased number of paths.

APPENDIX
DERIVATION OF (13) AND (14)

Taking the logarithm on both sides of (11) and letting

$$\begin{aligned} u &= \log_{10} p_B(b) \\ v &= \log_{10} b \end{aligned} \tag{A1}$$

the slope of the beampattern pdf $p_B(b)$ on the log–log plot can be calculated from (11) by

$$-\gamma = -\frac{du}{dv} = -\frac{1}{2}\frac{df_1}{dv} - \frac{df_2}{dv} - \frac{1}{2} \tag{A2}$$

where

$$f_1 = \log_{10}\left(1 - \frac{x^2}{(ka)^2}\right) \tag{A3}$$

$$f_2 = \log_{10}\frac{J_2(x)}{x^2}. \tag{A4}$$

Applying chain rule of derivatives, we have

$$\frac{d}{dv} = \frac{d}{dx}\frac{dx}{db}\frac{db}{dv} = \frac{b}{\log_{10}e}\frac{dx}{db}\frac{d}{dx} \tag{A5}$$

and from (7), the derivative dx/db is found to be

$$\frac{dx}{db} = \left(\frac{db}{dx}\right)^{-1} = -\left(\frac{8J_1(x)J_2(x)}{x^2}\right)^{-1}. \tag{A6}$$

In addition

$$\frac{df_1}{dx} = -\frac{2x}{(ka)^2 - x^2}\log_{10}e \tag{A7}$$

and

$$\frac{df_2}{dx} = -\frac{J_3(x)}{J_2(x)}\log_{10}e. \tag{A8}$$

Substituting (A6)–(A8) into (A2) and using (A5) leads to

$$\gamma = \left[\frac{x}{(ka)^2 - x^2} + \frac{J_3(x)}{J_2(x)}\right]\frac{bx^2}{8J_1(x)J_2(x)} + \frac{1}{2}. \tag{A9}$$

This is an exact expression for all values of the beampattern greater than the value of the highest sidelobe level. Below those values, the beampattern is multivalued and an analytical expression for γ is not practical to be derived.

For $x \ll 1$ or $b(x) \to 1$

$$\gamma = \frac{5}{6} + \frac{2}{(ka)^2}. \tag{A10}$$

ACKNOWLEDGMENT

The authors would like to thank S. Barkley of the Woods Hole Oceanographic Institution (WHOI), Woods Hole, MA, for her assistance in the preparation of the manuscript. They would also like to thank the anonymous reviewers for their suggestions.

REFERENCES

[1] P. Petitgas and J. J. Levenez, "Spatial organization of pelagic fish: Echogram structure, spatio-temporal condition, and biomass in senegalese waters," *ICES J. Mar. Sci.*, vol. 53, pp. 147–153, 1996.
[2] A. Okubo and S. A. Levin, *Diffusion and Ecological Problems: Modern Perspectives*. New York: Springer-Verlag, 2001, pp. 209–215.
[3] B. C. Heezen and C. D. Hollister, *The Face of the Deep*. New York: Oxford Univ. Press, 1971, ch. 10–13.
[4] N. P. Chotiros, H. Boehme, T. G. Goldsberry, S. P. Pitt, R. A. Lamb, A. L. Garcia, and R. A. Altenburg, "Acoustic backscattering at low grazing angles from the ocean bottom. Part II. Statistical characteristics of bottom backscatter at a shallow water site," *J. Acoust. Soc. Amer.*, vol. 77, pp. 975–982, 1985.
[5] T. K. Stanton and C. S. Clay, "Sonar echo statistics as a remote sensing tool: Volume and sea floor," *IEEE J. Ocean. Eng.*, vol. OE-11, no. 1, pp. 79–96, Jan. 1986.
[6] D. A. Abraham and A. P. Lyons, "Novel physical interpretations of K-distribution reverberation," *IEEE J. Ocean. Eng.*, vol. 27, no. 4, pp. 800–813, Oct. 2002.
[7] D. A. Abraham and A. P. Lyons, "Reverberation envelope statistics and their dependence on sonar bandwidth and scatterer size," *IEEE J. Ocean. Eng.*, vol. 29, no. 1, pp. 126–137, Jan. 2004.
[8] D. A. Abraham, "Array modeling of active sonar clutter," *IEEE J. Ocean. Eng.*, vol. 33, no. 2, pp. 158–170, Apr. 2008.
[9] D. A. Abraham and A. P. Lyons, "Simulation of non-Rayleigh reverberation and clutter," *IEEE J. Ocean. Eng.*, vol. 29, no. 2, pp. 347–362, Apr. 2004.
[10] T. K. Stanton, "Density estimates of biological sound scatterers using sonar echo peak PDF's," *J. Acoust. Soc. Amer.*, vol. 78, pp. 1868–1873, 1985.
[11] M. V. Trevorrow, D. L. Mackas, and M. C. Benfield, "Comparison of multifrequency acoustic and in situ measurements of zooplankton abundances in Knight Inlet, British Columbia," *J. Acoust. Soc. Amer.*, vol. 117, pp. 3574–3588, 2005.
[12] J. W. [Lord Rayleigh] Strutt, "Wave theory of light," *Phil. Mag.*, vol. 10, pp. 73–73, 1880.
[13] J. W. [Lord Rayleigh] Strutt, "On the problem of random vibrations in one, two, or three dimensions," *Phil. Mag.*, vol. 37, pp. 321–47, 1919.
[14] J. W. Goodman, *Statistical Optics*. New York: Wiley, 1985, ch. 2.
[15] V. V. Ol'shevskii, *Characteristics of Sea Reverberation*. New York: Consultants Bureau, 1967, ch. 3.
[16] T. C. Gallaudet and C. P. de Moustier, "High-frequency volume and boundary acoustic backscatter fluctuations in shallow water," *J. Acoust. Soc. Amer.*, vol. 114, pp. 707–725, 2003.
[17] M. Gensane, "A statistical study of acoustic signals backscattered from the sea bottom," *IEEE J. Ocean. Eng.*, vol. 14, no. 1, pp. 84–93, Jan. 1989.
[18] J. E. Ehrenberg, "A method for extracting the fish target strength distribution from acoustic echoes," in *Proc. Conf. Eng. Ocean Environ.*, 1972, vol. 1, pp. 61–64.
[19] J. E. Ehrenberg, T. J. Carlson, J. J. Traynor, and N. J. Williamson, "Indirect measurement of the mean acoustic backscattering cross section of fish," *J. Acoust. Soc. Amer.*, vol. 69, pp. 955–962, 1981.
[20] R. Barakat, "First-order statistics of combined random sinusoidal waves with applications to laser speckle patterns," *Optica Acta*, vol. 21, pp. 903–921, 1974.
[21] E. Jakeman and P. N. Pusey, "A model for non-Rayleigh sea echo," *IEEE Trans. Antennas Propag.*, vol. AP-24, no. 6, pp. 806–814, Nov. 1976.
[22] J. K. Jao and M. Elbaum, "First-order statistics of a non-Rayleigh fading signal and its detection," *Proc. IEEE*, vol. 66, no. 7, pp. 781–790, Jul. 1978.
[23] T. K. Stanton, D. Chu, and D. B. Reeder, "Non-Rayleigh acoustic scattering characteristics of individual fish and zooplankton," *IEEE J. Ocean. Eng.*, vol. 29, no. 2, pp. 260–268, Apr. 2004.
[24] E. Jakeman and R. J. A. Tough, "Non-Gaussian Models for the Statistics of Scattered Waves," in *Advances in Physics*. New York: Taylor & Francis, 1988, vol. 37, pp. 471–529.
[25] K. D. Ward, "Compound representation of high resolution sea clutter," *Electron. Lett.*, vol. 17, pp. 561–563, 1981.
[26] M. P. Wachowiak, R. Smolikova, J. M. Zurada, and A. S. Elmaghraby, "Estimation of K-distribution parameters using neural networks," *IEEE Trans. Biomed. Eng.*, vol. 49, no. 6, pp. 617–620, Jun. 2002.
[27] E. Jakeman, "On the statistics of K-distributed noise," *J. Phys. A, Math. Gen.*, vol. 13, pp. 31–48, 1980.
[28] E. Jakeman and R. J. A. Tough, "Generalized K distribution: A statistical model for weak scattering," *J. Opt. Soc. Amer.*, vol. 4, pp. 1764–1772, 1987.
[29] M. L. Peterson, C. S. Clay, and S. B. Brandt, "Acoustic estimates of fish density and scattering function," *J. Acoust. Soc. Amer.*, vol. 60, pp. 618–622, 1976.
[30] J. E. Ehrenberg, "A review of target strength estimation techniques," in *Underwater Acoustic Data Processing*, Y. Chan, Ed. Dordrecht, The Netherlands: Kluwer, 1989, pp. 161–175.
[31] L. E. Kinsler, A. R. Frey, A. B. Coppens, and J. V. Sanders, *Fundamentals of Acoustics*. New York: Wiley, 1982, ch. 8.
[32] C. S. Clay, "Deconvolution of the fish scattering PDF from the echo PDF for a single transducer sonar," *J. Acoust. Soc. Amer.*, vol. 73, pp. 1989–1994, 1983.
[33] T. K. Stanton and D. Chu, "Non-Rayleigh echoes from resolved individuals and patches of resonant fish at 2–4 kHz," *IEEE J. Ocean. Eng.*, vol. 35, no. 2, pp. 152–163, Apr. 2010.
[34] D. A. Abraham, "The effect of multipath on the envelope statistics of bottom clutter," *IEEE J. Ocean. Eng.*, vol. 32, no. 4, pp. 848–861, Oct. 2007.

Dezhang Chu received the B.A. degree in electrical engineering from the China University of Geosciences, Wuhan, China, in 1982 and the Ph.D. degree in geophysics from the University of Wisconsin, Madison, in 1989.

He was a Postdoctoral Scholar from 1989 to 1990 and a Postdoctoral Investigator from 1990 to 1991 with the Woods Hole Oceanographic Institution (WHOI), Woods Hole, MA. From 1991 to 2007, he was first a Research Associate and then a Research Specialist with the Department of Applied Ocean Physics and Engineering, WHOI. During that period at WHOI, he developed acoustic scattering models for zooplankton, fish, and seafloor, conducted laboratory and ocean measurements of scattering, as well as developed signal processing methods for acoustic scattering by marine organisms. From 2007 to present, he has been with the Acoustics Team of the NOAA/NMFS Northwest Fisheries Science Center (NWFSC), Fishery Resources Analysis and Monitoring Division, Seattle, WA. His research currently is focusing on acoustic scattering, characterization, and classification of fish.

Dr. Chu is a Fellow of the Acoustical Society of America.

Timothy K. Stanton received the B.S. degree from Oakland University, Rochester, MI, in 1974 and the M.S. and Ph.D. degrees from Brown University, Providence, RI, in 1977 and 1978, respectively, all in physics. His undergraduate research involved experiments in solid-state acoustics with Dr. N. Tepley as advisor and his graduate research involved nonlinear acoustics measurements and instrumentation development with Dr. R. Beyer as advisor.

From 1978 to 1980, he was a Senior Engineer with the Submarine Signal Division, Raytheon Company, Portsmouth, RI, where he was engaged in research, development, and testing of acoustic systems. From 1980 to 1988, he was a Member of the Scientific Staff, Department of Geology and Geophysics, University of Wisconsin, Madison, where he conducted various theoretical, laboratory, and field studies in acoustical oceanography with Dr. C. Clay. From 1988 to the present, he has been a Member of the Scientific Staff, Department of Applied Ocean Physics and Engineering, Woods Hole Oceanographic Institution (WHOI), Woods Hole, MA. From 1997 to 2001, he was Chair of the department and currently is a Senior Scientist. He currently is collaborating with colleagues in the development of models of acoustic scattering by marine organisms through various theoretical and laboratory methods, physics-based models of the statistics of scattered signals, and is applying the methods to ocean measurements. In addition to his research, he is part of the Massachusetts Institute of Technology (MIT), Cambridge, MA, and WHOI Joint Graduate Education Program and teaches acoustic scattering theory. Overall he has published papers covering the areas of nonlinear acoustics, acoustics instrumentation, fiber-optic hydrophones, echo statistics, and acoustic scattering by volumetric objects, seafloor, sea surface, and the underside of sea ice.

Dr. Stanton has served as Associate Editor for the *Journal of the Acoustical Society of America* and as a Guest Editor for a special issue of *Deep Sea Research*. He has also served as a Guest Editor for a special issue of the IEEE JOURNAL OF OCEANIC ENGINEERING. He is a Fellow of the Acoustical Society of America and is a Member of The Oceanography Society. In 1985, he was awarded the A.B. Wood medal for Distinguished Contributions to Underwater Acoustics.